

Remote trace gas quantification using thermal IR spectroscopy and digital filtering based on principal components of background scene clutter

Andreas Hayden, Robert Noll

Hughes Danbury Optical Systems, Inc., Danbury, CT 06810

ABSTRACT

For many years Hughes Danbury Optical Systems has been developing algorithms for detecting trace gases in the atmosphere using hyper-spectral data processing techniques. We have shown in the past that our Orthogonal Background Suppression (OBS) algorithms are effective for measuring the column density-thermal radiance contrast product of a gas plume in the atmosphere at some distance from a passive thermal-IR emission spectrometer. The algorithm facilitates the detection of the target signal in the presence of low signal to spectral clutter ratio. Our current work shows that using the non-linear absorption features of a target gases' spectral signature, coupled with our OBS algorithm, we can separate column density-thermal radiance contrast product and obtain absolute plume column density and plume temperature. The OBS algorithms are straight forward and allow detection near theoretical random noise limits. The efficacy of our novel technique is demonstrated using simulations and field data.

Keywords: trace gas detection, principal components, background suppression, linear filter

1. INTRODUCTION

There is a need by civilian and government agencies for a means of passively detecting and measuring trace gases in a plume, with sensors at some distance from the target plume. The sensor may be as close as the base of a smokestack monitoring the plume at the top, or it may be as far away as a satellite in orbit overhead. The techniques described in this paper may be used for remote monitoring of: adherence to environmental standards and regulations, process control, and local and global environmental conditions. Using an emission spectrometer coupled with our Orthogonal Background Suppression¹ (OBS) techniques we have been able to measure quantitatively the amount of trace gas in plume simulations and in field measurements.

In the trace effluent gas detection problem the spectral signal of interest is a small part of the overall signal measured by a spectral sensor. A basic correlation filter will have difficulty detecting the small target signal unless the background component of the measured spectrum is removed. Because of large variability among natural scene spectra, two spectrum differencing leaves a large residual which again masks the signal.

OBS is based on a simple assumption about background clutter that we have found to be surprisingly accurate. This assumption is that background spectral clutter can be assumed to be a linear combination of background spectra taken with no target gas in the field of view. OBS finds the proper combination of background scene components and removes them completely from the target spectrum leaving only the spectrum of the gas of interest and random noise.

One result of original OBS is an optimal linear filter able to suppress the large background component of a measurement and yield the column density-thermal radiance contrast product (DCP) of a gas plume in the atmosphere. Column density is the number of molecules per unit area seen by a sensor. Thermal radiance contrast is the difference between the radiance of the scene behind a plume and a Planck function generated with the temperature of the plume. However, original OBS could not separate column density from thermal radiance

contrast. In this paper we will demonstrate an enhancement to OBS which allows measurement of column density separately from thermal radiance contrast.

In the following sections we will review original OBS, outline the derivation of enhanced OBS, and give some examples of the effectiveness of the enhanced technique.

2. FORMULATION OF ORIGINAL OBS ORTHOGONAL FILTER

The theory, of both original OBS and the OBS enhancement described in this paper, is based on the viewing geometry schematically shown in figure 1. In this case the sensor is above the plume looking down through it to the ground. The simulations and data in this paper are based on this geometry.

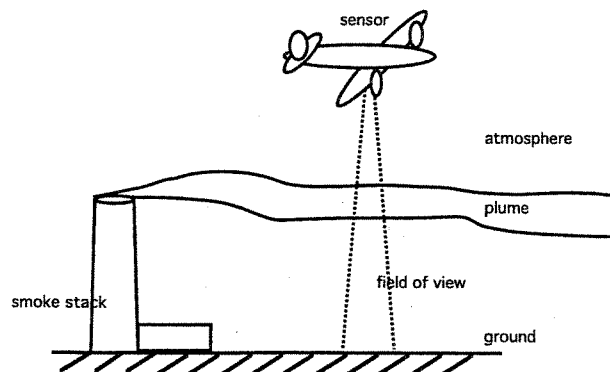


Figure 1. Schematic of measurement scenario. In a target pixel the sensor views the ground through intervening atmosphere and through the plume. In a background pixel (not shown in schematic), the sensor views ground through intervening atmosphere only.

The measured radiance in a target pixel can be expressed as a sum of: background radiance transmitted through the atmosphere, background radiance transmitted through the plume and through the atmosphere, plume radiance transmitted through the atmosphere, and atmospheric radiance (equation 1).

$$N_i^t = \underbrace{(1-f) N_i^g \tau_i^a}_{\text{background (not propagated through plume)}} + \underbrace{f N_i^g e^{-n_c \alpha_i} \tau_i^a}_{\text{background (propagated through plume)}} + \underbrace{f (1 - e^{-n_c \alpha_i}) B_i(T_p) \tau_i^a}_{\text{plume radiance}} + \underbrace{N_i^a}_{\text{atmospheric radiance}} \quad (1)$$

In equation 1: N_i^t is the measured target radiance, f is the fraction of the pixel filled by the plume, N_i^g is the radiance of the scene behind the plume, τ_i^a is the transmission of the atmosphere between the plume and the sensor, n_c is the column density, α_i is the absorption cross section of the molecule of interest, B is the Planck function, T_p is the plume temperature, and N_i^a is the radiance of the atmosphere between the plume and the sensor. The subscript "i" indicates that the quantities are arrays of values at varying wavenumber.

In original OBS the exponent terms (describing plume emissivity and plume transmittance) were expanded to first order (equation 2).

$$e^{-n_c \alpha_i} \approx 1 - n_c \alpha_i \quad (2)$$

This truncated expansion implicitly assumes that the plume is optically thin and that higher order terms are negligible.

Rewriting equation 1, using approximation 2, yields equation 3.

$$N_i^t = f \Delta b_i n_c \alpha_i \tau_i^a + N_i^s \tau_i^a + N_i^a \quad (3)$$

Δb is the thermal radiance contrast (equation 4).

$$\Delta b_i = B_i(T_p) - N_i^s \quad (4)$$

A more compact form of the equations is obtained if the spectra are expressed as n-dimensional vectors², where n is the number of wavelength samples in a spectrum. In vector notation equation 3 becomes equation 5.

$$N^t = f n_c \alpha \tau^a \Delta b + N^s \tau^a + N^a \quad (5)$$

OBS assumes that the background components of the target signal, represented by the last two terms in equations 3 and 5, can be expressed as a linear combination of a set of measured background pixels. The following paragraphs describe how the correct linear combination of backgrounds is found.

A set of basis vectors spanning the set of measured background spectra can be constructed using singular value decomposition^{3,4} (SVD) of the set of measured background spectra (equation 6).

$$B = U \Lambda V^T \quad (6)$$

B is the set of background spectra expressed as an array of vectors. **U** are the principal spectral components of the background set as found by SVD. Λ is the set of singular values describing the weights of the principal components. **V** is a "rotation matrix" describing how much of each principal component is in each background spectrum.

In our application the number of background spectra measured was fewer than the number of wavenumber samples in a spectrum. This does not lead to an under-constrained problem however. We have found that for a wide variety of scenarios the number of non-noise basis vectors in the spanning set is fewer than the number of background spectra in the measured background set. SVD is able to separate random noise degrees of freedom from actual scene spectral clutter components.

Our applications have been in the hyper to ultra spectral regimes ($n > 100$ wavelengths), both uplooking and down looking. We have found, in these regimes, that only on the order of 10 principal components are needed to completely describe all the non-noise background variability. This statement holds true when background spectra are taken close in time and space to target spectra. The number of principal components required can be determined by looking at the singular values generated during SVD. After a certain number of principal components the singular values stop decreasing rapidly, indicating that all subsequent principal components are describing noise.

The OBS assumption, that the background radiance in a target pixel is a linear sum of measured background spectra, means that equation 5 can be re-written as equation 7.

$$N^t = f n_c \alpha \tau^a \Delta b + U c \quad (7)$$

Where the background terms of equation 5 have been replaced by the linear sum of principal components, which are in turn a linear sum of the background spectra. The coefficient array **c** are the weights of the principal

components describing the background in the target pixel. We will use the orthonormality of U to find c and remove background components from the target spectrum.

In our earlier paper (reference 1) we showed that a vector could be constructed (equation 8) such that its normalized dot product with N^t yielded the $n_c \Delta b$ product (equation 9).

$$(\alpha \hat{\tau}^a)^\perp \equiv \alpha \hat{\tau}^a - U[U^T(\alpha \hat{\tau}^a)] \quad (8)$$

$$\frac{((\alpha \hat{\tau}^a)^\perp)^T}{((\alpha \hat{\tau}^a)^\perp)^T (\alpha \hat{\tau}^a)} N^t = n_c \Delta b \equiv DCP \quad (9)$$

The superscript T indicates vector or matrix transpose. The atmospheric transmission, $\hat{\tau}^a$, used in constructing the filter in equation 8 is an estimate based on knowledge of the atmospheric conditions during the measurements and is generated using FASCODE⁵.

In this paper we will show that OBS is able to separate n_c and Δb by using higher order terms in exponent expansion.

3. EXTENSION OF OBS TO MEASURE ABSOLUTE COLUMN DENSITY

3.1 Column Density Determination

If we expand equation 2 completely and combine it with equation 1 we get equation 10

$$N^t = f \Delta b \sum_{i=1}^{\infty} \left[\frac{(-1)^{(i+1)} n_c^i \alpha^i \tau^a}{i!} \right] + Uc \quad (10)$$

Originally Δb was treated as a constant. This worked for thin plume OBS. Simulations showed that for thick plumes there was coupling between higher order α terms and the Δb spectrum which caused errors in n_c determination. It was found that modeling Δb as a linear function of wavenumber (equation 11) allowed more accurate estimation of n_c .

$$\Delta b_i = \overline{\Delta b} + (\nu - \nu_i) b \quad (11)$$

In equation 11: $\overline{\Delta b}$, ν , b are constants and ν_i is the i^{th} wavenumber. The average thermal radiance contrast term, $\overline{\Delta b}$, is the thermal contrast constant of original OBS.

Rewriting equation 10, using equation 11 yields equation 12:

$$N^t = f \overline{\Delta b} \sum_{i=1}^{\infty} \left[\frac{(-1)^{(i+1)} n_c^i \alpha^i \tau^a}{i!} \right] + f \nu b \sum_{i=1}^{\infty} \left[\frac{(-1)^{(i+1)} n_c^i \alpha^i \tau^a}{i!} \right] - \nu b f \sum_{i=1}^{\infty} \left[\frac{(-1)^{(i+1)} n_c^i \alpha^i \tau^a}{i!} \right] + Uc \quad (12)$$

By analogy to equation 8 and 9, we would like to create a filter which when applied to equation 12 yields the coefficient of a particular α^i . In order to do this an augmented background set B' needs to be constructed (see equation 5) so that the basis set of vectors (U') spanning B' includes principal background components (U) as well as $(\omega^j \tau^a)$, and $(v \omega^j \tau^a)$ terms. Note that: $j \neq i$.

A filter for the coefficients of the α^i term is generated using equation 13.

$$(\alpha^i \hat{\tau}^a)^\perp \equiv \alpha^i \hat{\tau}^a - U' [U'^T (\alpha^i \hat{\tau}^a)] \quad (13)$$

The filter (equation 13) applied to equation 12, yields equation 14.

$$\frac{((\alpha^i \hat{\tau}^a)^\perp)^T}{((\alpha^i \hat{\tau}^a)^\perp)^T (\alpha^i \hat{\tau}^a)} N^t = f \overline{\Delta b} \frac{(-1)^{(i+1)} n_c^i}{i!} + f b \nabla \frac{(-1)^{(i+1)} n_c^i}{i!} - \frac{f b ((\alpha^i \hat{\tau}^a)^T (v \alpha^i \tau^a)) (-1)^{(i+1)} n_c^i}{((\alpha^i \hat{\tau}^a)^\perp)^T (\alpha^i \hat{\tau}^a) i!} \quad (14)$$

Note that $(\alpha^i \hat{\tau}^a)^\perp$ was constructed to cancel all ω^j terms in the absorption cross section spectra with $j \neq i$. Also, assuming $\hat{\tau}^a$ is a good approximation for τ^a and noting that the magnitude of the last two terms in equation 14 are nearly equal, yields equation 15

$$\frac{((\alpha^i \hat{\tau}^a)^\perp)^T}{((\alpha^i \hat{\tau}^a)^\perp)^T (\alpha^i \hat{\tau}^a)} N^t \approx f \overline{\Delta b} \frac{(-1)^{(i+1)} n_c^i}{i!} \quad (15)$$

Filtering for the coefficient of α yields:

$$\frac{((\alpha \hat{\tau}^a)^\perp)^T}{((\alpha \hat{\tau}^a)^\perp)^T (\alpha \hat{\tau}^a)} N^t = f \overline{\Delta b} n_c \quad (16)$$

Equation 16 and 17 are the original OBS result.

$$DCP_1 \equiv \frac{((\alpha \hat{\tau}^a)^\perp)^T}{((\alpha \hat{\tau}^a)^\perp)^T (\alpha \hat{\tau}^a)} N^t = f \overline{\Delta b} n_c \quad (17)$$

Filtering for the coefficient of α^2 yields:

$$DCP_2 \equiv \frac{((\alpha^2 \hat{\tau}^a)^\perp)^T}{((\alpha^2 \hat{\tau}^a)^\perp)^T (\alpha^2 \hat{\tau}^a)} N^t = f \overline{\Delta b} \frac{n_c^2}{2} \quad (18)$$

The estimate for plume column density is now simply:

$$\hat{n}_c = -2 \frac{DCP_2}{DCP_1} \quad (19)$$

Note that \hat{n}_c is a biased estimator for n_c for at least two reasons:

1) Because of system noise (assumed to be gaussian, white, and spectrally uncorrelated). The filtered measurements DCP_1 and DCP_2 will have some mean and variance. Even though DCP_1 and DCP_2 are random variables, they are correlated. The mean of the ratio of DCP_2/DCP_1 is not necessarily the ratio of the means of DCP_1 and DCP_2 .

2) Noise will "mask" higher order α terms. Further discussion of this point is in the Simulation Results section.

3.2 Effects of noise on n_c determination

An explicit noise term has been left out of the foregoing equations. When a spectrum is measured it will include the radiances described in equation 1 plus a vector of random noise. We assume the noise in each wavenumber bin is zero mean, gaussian, uncorrelated, and has a standard deviation equal to noise equivalent spectral radiance (NESR). When the linear filters described in equations 17 and 18 are applied to an ensemble of these random spectra the standard deviation of the results are the noise equivalent density contrast products, NE_{DCP1} and NE_{DCP2} .

$$NE_{DCP1} = \frac{NESR}{\left[\left((\alpha \hat{\tau})^\perp \right)^T (\alpha \hat{\tau}) \right]^{\frac{1}{2}}} \quad (20)$$

$$NE_{DCP2} = \frac{NESR}{\left[\left((\alpha^2 \hat{\tau})^\perp \right)^T (\alpha^2 \hat{\tau}) \right]^{\frac{1}{2}}} \quad (21)$$

The noise equivalent n_c (NE_{nc}) is the standard deviation of the ratio:

$$\hat{n}_c \pm NE_{nc} = -2 \frac{DCP_2 \pm NE_{DCP2}}{DCP_1 \pm NE_{DCP1}} \quad (22)$$

Therefore⁶:

$$NE_{nc} = 2 \left[\frac{(DCP_2 NE_{DCP1})^2}{DCP_1^4} + \frac{NE_{DCP2}^2}{DCP_1^2} \right]^{\frac{1}{2}} \quad (23)$$

3.3 Plume temperature determination

The thermal radiance contrast can be estimated using DCP_1 and DCP_2 in a fashion similar to n_c determination (equation 24).

$$\Delta b = - \frac{DCP_1^2}{2 \hat{f} DCP_2} \quad (24)$$

Where \hat{f} is an estimate of the plume fill factor.

To get plume temperature from the thermal radiance contrast we need an estimate of the ground radiance, N^8 . Equation 25 can then be solved for T_p , (equation 26).

$$\overline{\Delta b} = B_v(T_p) - \widehat{N}_i^s \quad (25)$$

$$T_p = \frac{c_2 \nabla}{\ln \left(\frac{c_1 \nabla^3}{(\overline{\Delta b} + \widehat{N}_i^s) + 1} \right)} \quad (26)$$

Where B_v is the value of Planck's function at the spectral window's average wavelength, \widehat{N}_i^s is the estimated average background radiance in the target pixel, c_1 and c_2 are the coefficients of Planck's equation.

4. SIMULATION RESULTS

Figure 2 shows a simulated SO_2 plume spectrum. We will use enhanced OBS to extract the n_c of SO_2 in this spectrum.

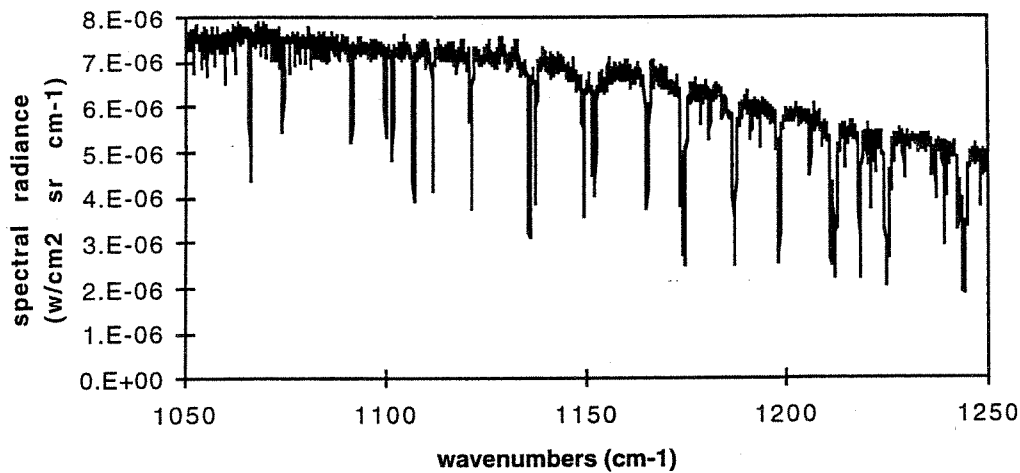


Figure 2. Simulated SO_2 plume spectrum. Simulates downlooking from 4.5 km and includes: ground radiance, plume radiance and transmission, atmospheric radiance and transmission, and white noise.

The parameters used to generate the spectrum shown in figure 2 are listed in table 1.

n_c of SO_2	1×10^{19} molecule/ cm^{-2}
T_p	305K
T_g	295K
ground emissivity	1
fill factor	1
atmosphere model	mid-latitude winter
sensor altitude	4.5 km (nadir view)
NESR	1×10^{-7} w/ cm^2 sr cm^{-1}

Table 1. Parameters of simulated target plume.

The backgrounds for the simulation were a set of black body spectra generated with ground temperature varying from 290K to 300K. The peak target signal to NESR ratio in the target pixel is 10. The peak target signal to scene clutter ratio is 1/7.

Figure 3 shows the molecular absorption cross-section of SO₂ used to construct the SO₂ filter. Note that visually the SO₂ features are almost completely obscured by the spectral clutter in the target spectrum (figure 2).

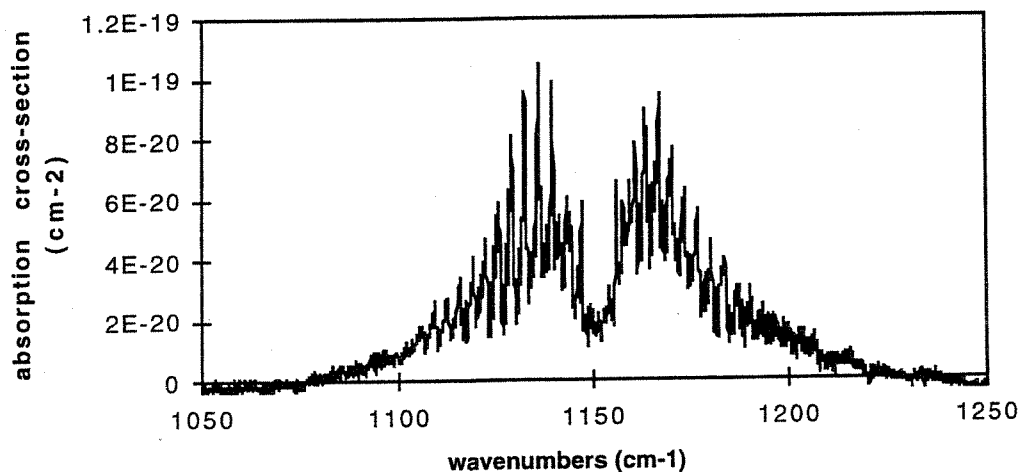


Figure 3. Molecular absorption cross-section (α) of SO₂.

Figure 4 shows filter results for the simulated SO₂ plume. The x-axis is number of α^i terms added to the augmented background set **B'**. For example, if the number of α^i terms indicated is 2 then **B'** includes: the non-noise background principal components, ($\alpha^2 \tau^a$), and ($v \alpha^2 \tau^a$). The error bars indicate the noise equivalent column density (NE_{nc}).

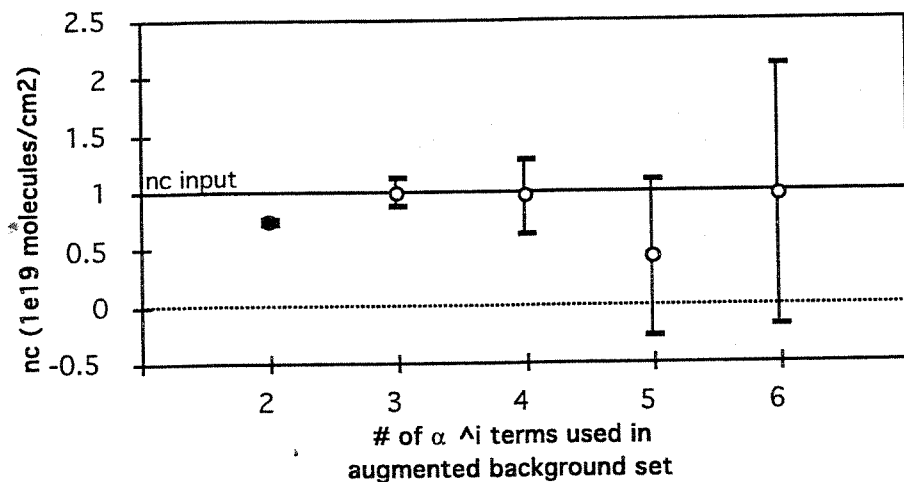


Figure 4. Estimated n_c results (based on simulation) versus number of terms included in augmented background set. Error bars indicate NE_{nc}. Amount of SO₂ in plume is indicated by the line "nc input".

The plot in figure 4 starts with α^2 added to B' since at least two terms are required in the expansion to determine n_c .

As number of terms used to generate filter increases the estimated value of n_c approaches the input value. But, at the same time, noise equivalent n_c (NE_{nc}) increases. There is a number of terms where the best estimate of n_c is found. This estimate will be biased by the early cutoff of expansion terms.

5. FIELD DATA RESULTS

We received data taken with the JPL Airborne Emission Spectrometer⁷ (AES) of a plume from a smokestack. The altitude of the sensor was 15,000 ft and was nadir viewing. The data we received were calibrated in units of $\text{watts/cm}^2 \text{ sr cm}^{-1}$. We windowed the spectra to $1050\text{--}1250 \text{ cm}^{-1}$ since we were looking specifically for SO_2 measurements.

The sensor is a linear array of 4 detectors which can be push-broomed to build a $4 \times m$ ultra-spectral image (m is the number of scans in a run). The sensor can also track a stationary target on the ground as the aircraft flies over. During scans 1-9 the sensor was push-broomed across the ground leading up to the target smokestack. These 36 spectra comprised the original background set, B . During scans 9-28 the sensor locked on to the stack and viewed the plume from various angles as the aircraft flew over.

Figure 5 shows example of a target spectrum.

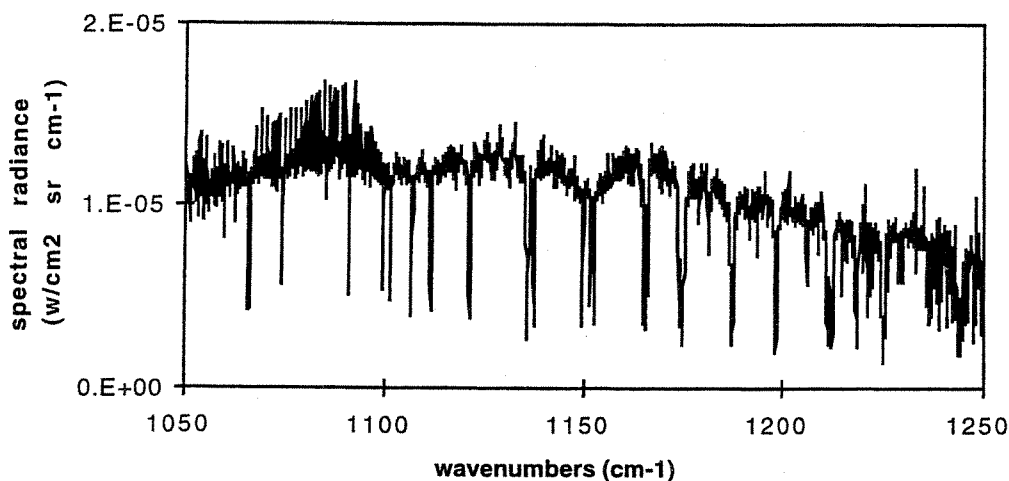


Figure 5. Example target spectrum from field data. Smokestack plume spectral radiance.

The emission feature between 1050 cm^{-1} and 1100 cm^{-1} is hot CO_2 which is also an effluent from the stack. If the CO_2 is not accounted for in constructing a filter for SO_2 the filter may couple with the CO_2 feature and give an incorrect SO_2 measurement result. To account for interferent gases (e.g., in this case, CO_2) the absorption spectrum of a suspected interferent is added to the augmented background set, B' . When a spectrum is added to B' the filter constructed from B' will not correlate with that spectrum. With CO_2 added to B' the CO_2 emission will not interfere with the SO_2 measurement.

Figure 6 shows n_c estimates, calculated NE_{nc} and ground truth estimates for SO_2 column density in the plume.

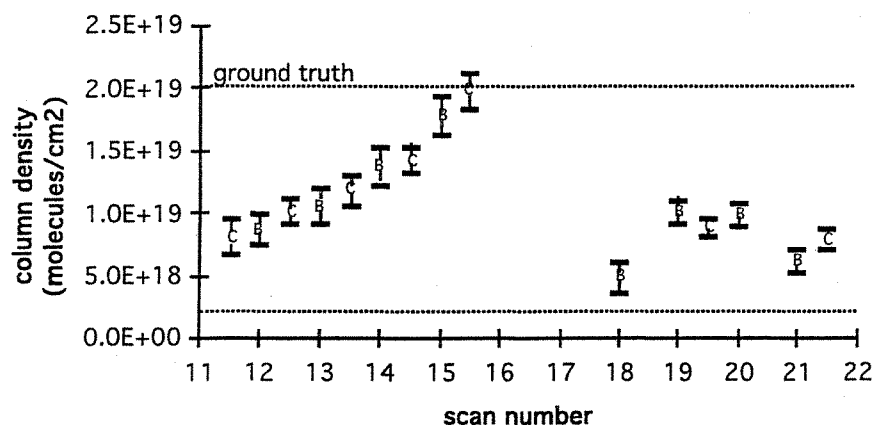


Figure 6. Measured field data. Column density versus scan number (pixel for which measurement was made indicated by letter). Range of ground truth estimate indicated by horizontal lines.

The error bars indicate only the NE_{nc} and do not take into account any other possible systematic errors. The ground truth estimate range is indicated by the horizontal lines.

Scans 1-9 were used as background so no SO_2 measurements are shown for them. In scans 10, and after 21 the plume was either too thin or the thermal contrast too low to be able to make column density measurements (even though for those scans SO_2 could be detected). In scans 16 and 17 the plume was being viewed against the hot roof of a building. In these two scans the plume was about the same temperature as the background, so the thermal contrast was too low to make column density measurements.

6. SUMMARY

OBS is a linear filtering technique based on the assumption that background scene components in a target pixel are a linear sum of measured scene background spectra. A linear filter can be constructed to reject background scene components and yield plume gas column density-thermal radiance contrast products. If filters for various powers of target gas absorption spectra are constructed, absolute column density and plume temperature can be separately determined.

Further work should include a more rigorous derivation of the orthogonal filters and of the statistics of the resulting measurements. More data with tighter control over the ground truth should be processed.

7. REFERENCES

1. A. Hayden, E. Niple, B. Boyce, "Determination of trace-gas amounts in plumes by use of orthogonal digital filtering of thermal-emission spectra," *Appl. Opt.* 35, 2802-2809 (1996).
2. Morgan, D. R. "Spectral Absorption Pattern Detection and Estimation." *Applied Spectroscopy*, 31, 5, 404-424 (1977).
3. Golub, G. H. Matrix Computations. (Johns Hopkins University Press, Baltimore, 1983).
4. W. H. Press, S. A. Teukolsky, W. T. Vetterling, B. P. Flannery, Numerical Recipes in C, (Cambridge University Press, New York, 1992), p. 59.

5. H. J. P. Smith, D. J. Dube, M. E. Gardner, S. A. Clough, F. X. Kneizys, L. S. Rothman, "FASCODE-Fast Atmospheric Signature Code (Spectral Transmittance and Radiance)," AFGL-TR-78-0081 (Air Force Geophysics Laboratory, Bedford, MA 01731, 1978).

6. A. C. Melissinos, Experiments in Modern Physics, (Academic Press, Inc., New York, 1966), p. 469.

7. D. M. Rider, R. Beer, J. S. Margolis, H. Worden, S. Sumita, T. Glavich, "Airborne emission spectrometer: a testbed for the EOS TES," Proc. SPIE, 2820, 1996.